Cancer Cell
Article

Tumor-Targeted Interferon-α Delivery by Tie2-Expressing Monocytes Inhibits Tumor Growth and Metastasis

Michele De Palma,[1,2,8,*] Roberta Mazzieri,[1,2,8] Letterio S. Politi,[5] Ferdinando Pucci,[1,2,6] Erika Zonari,[1,2] Giovanni Sitia,[3] Stefania Mazzoleni,[4] Davide Moi,[1,2] Mary Anna Venneri,[1,2] Stefano Indraccolo,[7] Andrea Falini,[5] Luca G. Guidotti,[3] Rossella Galli,[4] and Luigi Naldini[1,2,6,*]
[1]Angiogenesis and Tumor Targeting Research Unit
[2]San Raffaele Telethon Institute for Gene Therapy (HSR-TIGET)
[3]Immunopathogenesis of Liver Infections Unit
[4]Stem Cell Research Institute
San Raffaele Institute, 20132 Milano, Italy
[5]Neuroradiology Division, Head and Neck Department, and CERMAC, San Raffaele Hospital, 20132 Milano, Italy
[6]Vita-Salute San Raffaele University Medical School, 20132 Milano, Italy
[7]Istituto Oncologico Veneto–IRCCS, 35128 Padova, Italy
[8]These authors contributed equally to this work
*Correspondence: depalma.michele@hsr.it (M.D.P.), naldini.luigi@hsr.it (L.N.)
DOI 10.1016/j.ccr.2008.09.004

SUMMARY

The use of type I interferons (IFNs) in cancer therapy has been limited by ineffective dosing and significant toxicity. Here, we exploited the tumor-homing ability of proangiogenic Tie2-expressing monocytes (TEMs) to deliver IFN-α to tumors. By transplanting hematopoietic progenitors transduced with a *Tie2* promoter/enhancer-driven *Ifna1* gene, we turned TEMs into IFN-α cell vehicles that efficiently targeted the IFN response to orthotopic human gliomas and spontaneous mouse mammary carcinomas and obtained significant antitumor responses and near complete abrogation of metastasis. TEM-mediated IFN-α delivery inhibited tumor angiogenesis and activated innate and adaptive immune cells but did not impair myelopoiesis and wound healing detectably. These results illustrate the therapeutic potential of gene- and cell-based IFN-α delivery and should allow the development of IFN treatments that more effectively treat cancer.

INTRODUCTION

Type I interferons (IFN-α and -β) are highly pleiotropic cytokines—produced by virtually every vertebrate cell—that play important functions in protecting the host from viral infections (Parmar and Platanias, 2003; Stark et al., 1998; Stetson and Medzhitov, 2006). As early as 1969, it was shown that these cytokines also have antitumor activity. Indeed, mice inoculated with syngeneic tumor cells exhibited significantly increased survival when treated with type I IFN preparations (Gresser et al., 1969). This seminal study triggered a wealth of research eventually leading to clinical testing of type I IFNs in cancer therapy (Belardelli et al., 2002; Brassard et al., 2002).

IFN-α was the first cytokine to show clinical benefit in the treatment of certain types of cancer, including melanoma, chronic myelogenous leukemia, and renal cancer. High doses of IFN-α are required to obtain therapeutic responses in cancer patients; however, these regimens are highly toxic, and the clinical use of IFN-α has been progressively phased out as alternative pharmacological treatments have became available (Belardelli et al.,

SIGNIFICANCE

IFN-α was the first cytokine approved for cancer treatment. However, given the limited efficacy and significant toxicity associated with systemic IFN-α administration, delivery strategies that improve IFN-α therapeutic index are required. Here, IFN-α delivery by gene-modified Tie2-expressing monocytes (TEMs) achieved substantial antitumor activity in both prevention and intervention trials but did not cause measurable toxicity. Conversely, expression of IFN-α broadly in hematopoietic cells or in plasma was highly toxic and, paradoxically, poorly effective. Because stromal cells are the crucial targets of IFN-α in tumors, resistance to this therapy is unlikely to develop. Hematopoietic progenitors engineered to express IFN-α specifically in TEM progeny might be administered together with unmodified cells in the setting of autologous bone marrow transplantation in cancer patients receiving high-dose chemotherapy.

2002; Brassard et al., 2002; Gutterman, 1994; Parmar and Platanias, 2003). Concerning the mechanisms of antitumor activity, type I IFNs were long thought to act mainly by suppressing tumor cell proliferation and angiogenesis (Pfeffer, 1997; Sidky and Borden, 1987). These cytokines can directly promote apoptosis of tumor and stromal cells and may inhibit angiogenesis by downregulating the expression of proangiogenic factors in tumors. More recently, it has been established that IFN-α and -β also have important roles in regulating the innate and adaptive arms of the immune system. Indeed, type I IFNs activate dendritic cells (DCs); upregulate the expression of major histocompatibility complex (MHC) class I molecules; promote the priming and survival of T cells; enhance humoral immunity; and increase the cytotoxic activity of natural killer (NK) cells, macrophages, and $CD8^+$ T cells. Moreover, they increase the susceptibility of target cells (both tumor and stromal cells) to the cytotoxic activities of immune effectors. Through these immunomodulatory functions, type I IFNs increase tumor immunogenicity, recruit and activate immune cells within the tumor milieu, and may eventually facilitate tumor rejection (Belardelli et al., 2002; Blankenstein, 2005; Brassard et al., 2002; Dunn et al., 2006; Theofilopoulos et al., 2005; Willimsky and Blankenstein, 2007). Recent studies have further shown that IFN responsiveness in the host hematopoietic compartment is necessary and sufficient to evoke antitumor activity, suggesting that the crucial targets of IFN responses are the host cells rather than the tumor cells (Dunn et al., 2006). Thus, by exerting antiproliferative, angiostatic, and immune cell-activating functions, type I IFNs likely play a vital role in tumor growth control. Nevertheless, the overall limited therapeutic efficacy of current treatments based on type I IFNs might reflect our inability to target these potent antitumor molecules to the right place and/or at the right dose. Alternative delivery strategies are thus needed to achieve safe and effective IFN delivery in cancer patients.

High-dose chemotherapy followed by adjuvant autologous hematopoietic stem/progenitor cell (HSPC) transplantation has been tested for the treatment of hematological and solid tumors and can be regarded as a clinical option for certain types of cancer (Fuchs and Whartenby, 2004; Ljungman et al., 2006). As viral gene transfer strategies become better suited to the clinic, approaches based on transplantation of genetically modified HSPCs have the potential to increase significantly the therapeutic efficacy of standard cancer therapies. We and others have recently highlighted the important contribution of bone marrow (BM)-derived myeloid cells to tumor angiogenesis (de Visser et al., 2006; Condeelis and Pollard, 2006; De Palma et al., 2007; De Palma and Naldini, 2006; Shojaei et al., 2008). We identified, in both mice and humans, a subset of circulating and tumor-infiltrating monocytes that express the angiopoietin receptor Tie2 (Jones et al., 2001) and are proangiogenic. These Tie2-expressing monocytes (TEMs) are effectively recruited to tumors, where they play an important role in neoangiogenesis, but are infrequently found in normal organs (De Palma et al., 2003, 2005b, 2007; Venneri et al., 2007; Ahn and Brown, 2008; Du et al., 2008). Based on this unique tumor-homing specificity among myeloid-lineage cells and the selective expression of the *Tie2* gene in TEMs among the progeny of BM-derived HSPCs, we explored the possibility of targeting IFN-α to tumors by expressing it in TEMs from a lentiviral vector (LV) regulated by *Tie2* promoter/enhancer elements (De Palma et al., 2003). By this strategy, we turned proangiogenic monocytes into tumor-selective IFN-α delivery vehicles and achieved significant antitumor activity in orthotopic, spontaneous, and metastatic models of oncogenesis.

RESULTS

Generation of Mice with TEM-Specific Expression of an *Ifna1* Transgene and Inhibition of Orthotopic Human Gliomas

We constructed LVs expressing a mouse *Ifna1* cDNA either from promoter/enhancer sequences of the *Tie2* gene (Tie2-IFN LV) or from the ubiquitously active phosphoglycerate kinase (*PGK*) promoter (PGK-IFN LV). We then transduced HSPCs obtained from the BM of CD1 athymic (*nu/nu*) mice with either type of LV and transplanted the transduced cells into lethally irradiated mice to obtain mice with TEM-specific (Tie2-IFN mice) or panhematopoietic (PGK-IFN mice) IFN-α expression, respectively. As controls, we transplanted mice with HSPCs transduced with Tie2-GFP or PGK-GFP control LVs to obtain Tie2-GFP and PGK-GFP mice, respectively. A schematic of the experimental design is shown in Figure 1A.

In liquid culture, HSPCs transduced with the Tie2-IFN LV expressed IFN-α to a much lower extent than PGK-IFN LV-transduced cells (Figure 1B). This was consistent with the frequency and mean fluorescence intensity (MFI) of GFP^+ cells among HSPCs transduced with the control Tie2-GFP and PGK-GFP LVs (Figure 1C). HSPCs transduced with the PGK-IFN LV did not engraft in lethally irradiated mice, which died 10–12 days after the transplant with overt BM aplasia (Figure 1D). In contrast, Tie2-IFN mice were reconstituted long-term by gene-modified cells (average vector copy number per cell 0.6 ± 0.2) and recovered normal blood cell and platelet counts, hemoglobin, and hematocrit (Figure 1E), and all survived until the end of the experiments. Despite the long-term engraftment of gene-modified cells, IFN-α was not detectable in the plasma of Tie2-IFN mice by ELISA (data not shown). This latter finding is consistent with the minimal expression of *Tie2* promoter/enhancer-driven transgenes in the hematopoietic system. Indeed, in Tie2-GFP mice, GFP^+ cells were only 3%–6% of the total BM cells (Figure 1F) and 1%–2% of the total leukocytes in the blood, identified as monocytes by the expression of CD11b and their physical parameters (Figure 1G). Together, these results show that the *Ifna1* transgene, when expressed from *Tie2* transcription elements in the hematopoietic system, does not interfere with HSPC engraftment and does not yield systemic IFN-α expression from the reconstituted transgenic hematopoietic cells.

We inoculated U87 human glioma cells intracranially in Tie2-IFN (n = 10) and control Tie2-GFP (n = 5) and PGK-GFP (n = 7) athymic mice 8 weeks after the transplant of the gene-modified HSPCs and monitored tumor growth by magnetic resonance imaging (MRI) for up to 5 weeks post tumor injection (PTI) (Figure 2). Three weeks PTI, tumor volume reached 24.6 ± 4.3 mm^3 in control mice (including Tie2-GFP and PGK-GFP mice), whereas it was only 3.8 ± 2.1 mm^3 in Tie2-IFN mice (Figure 2A). Of note, the majority of Tie2-IFN mice were either tumor-free or had tumors barely detectable by MRI at 4 or 5 weeks PTI, whereas all control mice carried large tumors and had to be euthanized by this time (Figures 2A–2C and data not shown). Despite their small

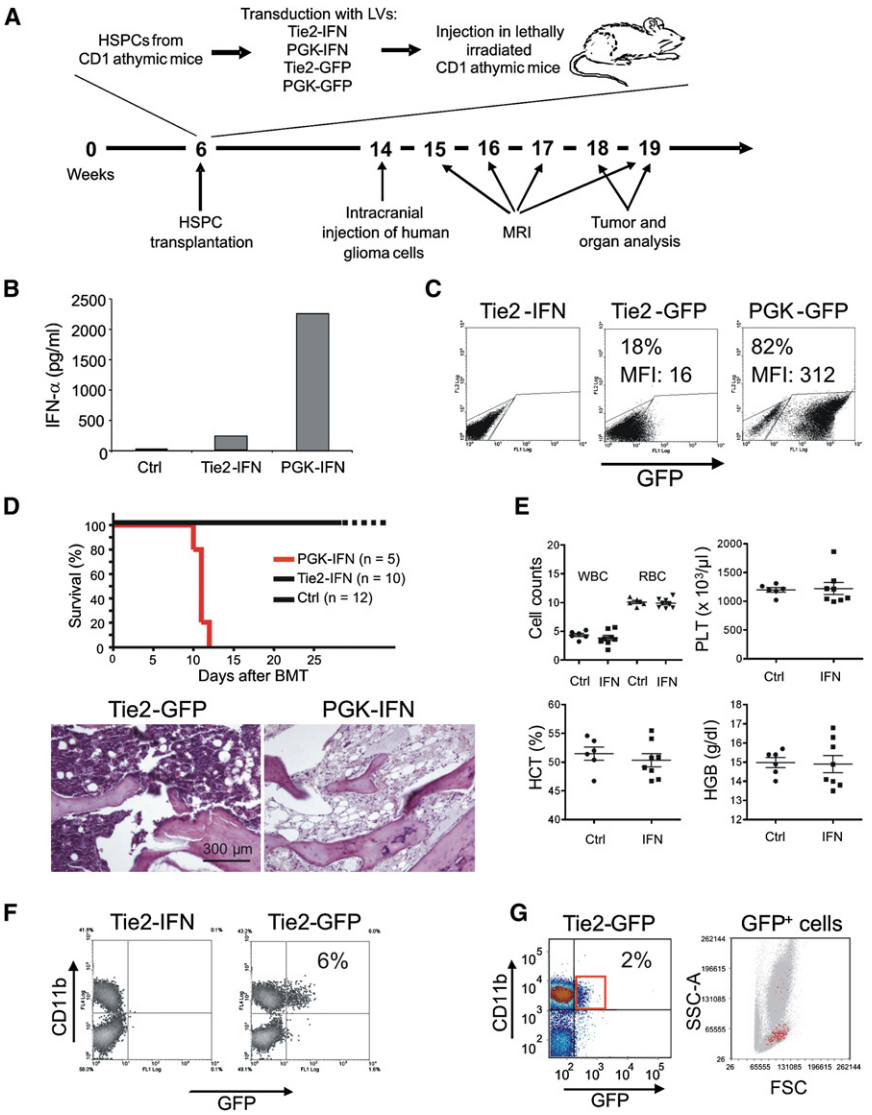

Figure 1. Generation of CD1 Athymic Mice with TEM-Specific Expression of an *Ifna1* Transgene

(A) Schematic of the experimental design.

(B) IFN-α expression by bone marrow (BM)-derived hematopoietic stem/progenitor cells (HSPCs), transduced with control (Ctrl) Tie2-GFP, Tie2-IFN, and PGK-IFN lentiviral vectors (LVs) and expanded in vitro for 9 days. One experiment representative of three independent experiments is shown.

(C) GFP expression in transduced HSPCs after 5 days of culture. The percentage and the mean fluorescence intensity (MFI) of the GFP$^+$ cells are indicated. One experiment representative of six independent experiments is shown.

(D) Top: survival curves of HSPC-transplanted mice. Control mice (Ctrl) include both Tie2-GFP and PGK-GFP mice. Bottom: hematoxylin and eosin (H&E) staining of whole BM (femur) of representative control (Tie2-GFP; n = 2) and PGK-IFN (n = 3) mice analyzed at day 12 posttransplant.

(E) Blood cell counts and hematological parameters (mean ± SEM) in HSPC-transplanted control (Ctrl; n = 6) and Tie2-IFN (IFN; n = 8) mice. WBC, white blood cells (×10^3/μl); RBC, red blood cells (×10^6/μl); PLT, platelets; HCT, hematocrit; HGB, hemoglobin.

(F) FACS analysis of BM cells from representative Tie2-IFN and Tie2-GFP mice, performed 13 weeks after HSPC transplantation. The percentage of GFP$^+$CD11b$^+$ myeloid cells is indicated. One experiment representative of several independent experiments is shown.

(G) FACS analysis of peripheral blood from a representative Tie2-GFP mouse. The GFP$^+$ cells are virtually all CD11b$^+$ (red gate in left panel) and have light scattering features of monocytes (right panel). One experiment representative of several independent experiments is shown.

size, tumors detectable in Tie2-IFN mice appeared more necrotic than those of control mice as measured by MRI at 3 weeks PTI (Figure 2D). The Tie2-IFN tumors that grew sufficiently to be analyzed displayed decreased cell proliferation and greater apoptosis (assessed by Ki-67 and cleaved caspase-3 immunostaining, respectively) as compared to the control tumors (Figure 2E).

In agreement with our previous findings (De Palma et al., 2007), GFP$^+$ TEMs surrounded angiogenic blood vessels in control Tie2-GFP tumors (Figure 3A). TEMs were CD11b$^+$ but could be distinguished from tumor-associated macrophages (CD11b$^+$GFP$^-$) by their small, rounded shape and their preferential position around blood vessels. Anti-IFN-α antibodies detected several mononuclear cells strongly positive for IFN-α (IFN-α^{bright}) in the gliomas of Tie2-IFN mice, but not of control mice (Figure 3A and data not shown). The frequency and distribution of IFN-α^{bright} cells in Tie2-IFN tumors were similar to those of GFP$^+$ TEMs in control tumors, suggesting that the IFN-α^{bright} cells represent bona fide IFN-producing TEMs.

Tie2-IFN tumors, but not control tumors, were heavily surrounded and infiltrated by cells expressing Iba1 (Figure 3B), a monocyte/macrophage/microglia protein upregulated upon cell activation and involved in cell migration and phagocytosis (Deininger et al., 2002). We previously showed that in these experimental conditions, the wide majority of glioma-infiltrating hematopoietic cells are of BM origin and express F4/80, thus representing tumor-associated macrophages (De Palma et al., 2005b). Together, these results suggest that the Iba1-expressing cells in Tie2-IFN tumors represent macrophages activated by IFN signaling. We then analyzed the expression of a panel of IFN-α-inducible genes (Honda et al., 2005; Stark et al., 1998) in the tumors. RNase protection assays (RPA) performed using a set of mouse-specific probes showed that IFN-responsive genes were strongly upregulated in the gliomas of Tie2-IFN mice as compared to control tumors or brain tissue obtained from the contralateral, noninjected brain hemisphere (Figure 3C). In particular, 2′5′-oligoadenylate synthetase (*Oas1a*, a prototypical IFN-inducible gene), tumor necrosis factor-α (*Tnfa*), and interleukin-1α and -1β (*Il1a/b*), all typical indicators of type I IFN-induced responses, were significantly upregulated in Tie2-IFN tumors. These findings indicated expression of biologically

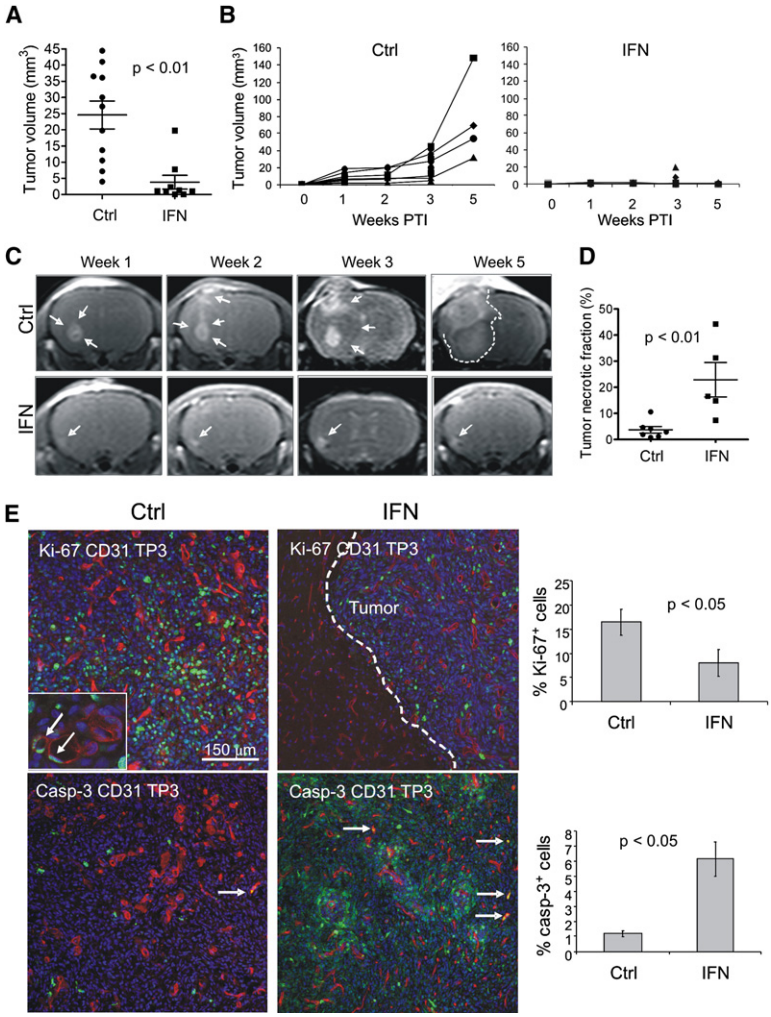

Figure 2. Inhibition of Orthotopic Human Gliomas in Tie2-IFN Athymic Mice

(A) Glioma growth (mean tumor volume ± SEM, measured by MRI) in individual control (Ctrl; n = 11 of 12) and Tie2-IFN (IFN; n = 9 of 10) mice at 3 weeks post tumor injection (PTI). Ctrl mice include both Tie2-GFP (n = 5) and PGK-GFP (n = 6) mice.

(B) Glioma growth in individual mice from week 1 to week 5 PTI. Note that 4 Tie2-IFN and 5 control mice were euthanized at 4 weeks PTI for further analyses.

(C) Contrast-enhanced T1-weighted (week 1, 2, and 5) and T2-weighted (week 3) coronal MRI images showing brain tumor growth at the indicated time points PTI in representative control PGK-GFP (Ctrl) and Tie2-IFN (IFN) mice. Intracranial gliomas are indicated by arrows and dashed line.

(D) Tumor necrotic fraction (mean necrotic fraction, % ± SEM) by MRI in individual control (Ctrl; n = 7) and Tie2-IFN (IFN; n = 5) mice at 3 weeks PTI.

(E) Ki-67 or caspase-3 (Casp-3; green) and CD31 (red) immunostaining and TO-PRO-3 (TP3) nuclear staining (blue) of intracranial gliomas grown in control Tie2-GFP (Ctrl) and Tie2-IFN (IFN) mice. Arrows show Ki-67$^+$CD31$^+$ or caspase-3$^+$CD31$^+$ endothelial cells (ECs); dashed line indicates tumor margin. Brain sections were analyzed at 4 or 5 weeks PTI. Histograms at right show quantification (mean frequency of marker-positive cells, % ± SD; n = 3–5) of Ki-67$^+$ or caspase-3$^+$ cells.

active concentrations of IFN-α at the tumor site in Tie2-IFN mice. IFNs display species specificity of action (Balkwill and Proietti, 1986; Sidky and Borden, 1987). Accordingly, we found that murine IFN-α inhibited the proliferation of murine cell lines but not human glioma cells in vitro (see Figure S1 available online). When we performed RPA using human-specific probes, we did not detect significant expression of IFN-inducible genes in Tie2-IFN gliomas, indicating that the IFN pathway was minimally activated in the tumor cells of human origin (Figure 3C). These results indicate that an IFN response targeted to the host-derived components of the tumor is capable of inhibiting human glioma growth in the mouse brain.

We then studied tumor angiogenesis. There were striking differences in the vascularization of control and Tie2-IFN gliomas (Figure 4A). Whereas the blood vessels of control tumors were notably enlarged and tortuous, those of Tie2-IFN tumors were small, had a regular profile, and were richly covered by NG2$^+$ pericytes, all typical features of quiescent or "normalized" blood vessels. The relative vascular area of Tie2-IFN tumors was only 33% of that of control tumors, and the blood vessels of Tie2-IFN tumors contained fewer Ki-67$^+$ proliferating endothelial cells (ECs) and increased numbers of caspase-3$^+$ apoptotic cells compared to those of control tumors (Figure 4B). Together, these findings strongly suggest that blood vessels of Tie2-IFN gliomas are in a quiescent, nonangiogenic state.

Tumor Growth and Myelotoxicity in Mice Expressing Systemic IFN-α

In order to better assess the advantages of targeted delivery, we studied the safety and efficacy of IFN-α in a model of systemic administration. To obtain mice with systemic IFN-α expression (s-IFN mice), we intravenously injected a group of Tie2-GFP mice with PGK-IFN LVs. By intravenous injection, LVs preferentially transduce the liver and the spleen, where they establish a stable source of the transgene product (Brown et al., 2006). Three weeks following LV injection, s-IFN mice expressed easily detectable IFN-α in the plasma (418 ± 124 pg/ml; mean ± SD; n = 4) as measured by ELISA. In this model of systemic expression, IFN-α failed to inhibit glioma growth and induced myelotoxicity with marked thrombocytopenia (Figure S2). Moreover, systemic IFN-α induced progressive body weight loss in s-IFN mice (data not shown). In agreement with these observations, elevated doses of IFN-α have suppressive effects on hematopoiesis and are toxic in humans (Belardelli et al., 2002; Parmar and Platanias, 2003). Together with the data of Figures 1–4 above, these results show that tumor-targeted IFN-α delivery by TEMs, but not its ubiquitous expression in BM-derived cells or sustained expression in the plasma, achieves substantial antitumor activity in an orthotopic human glioma model without inducing systemic toxicity.

Preferential Activation of the *Tie2* Promoter/Enhancer in the Tumor Microenvironment

It may appear difficult to reconcile the lack of myelotoxicity with the strong antitumor effects observed in Tie2-IFN mice.

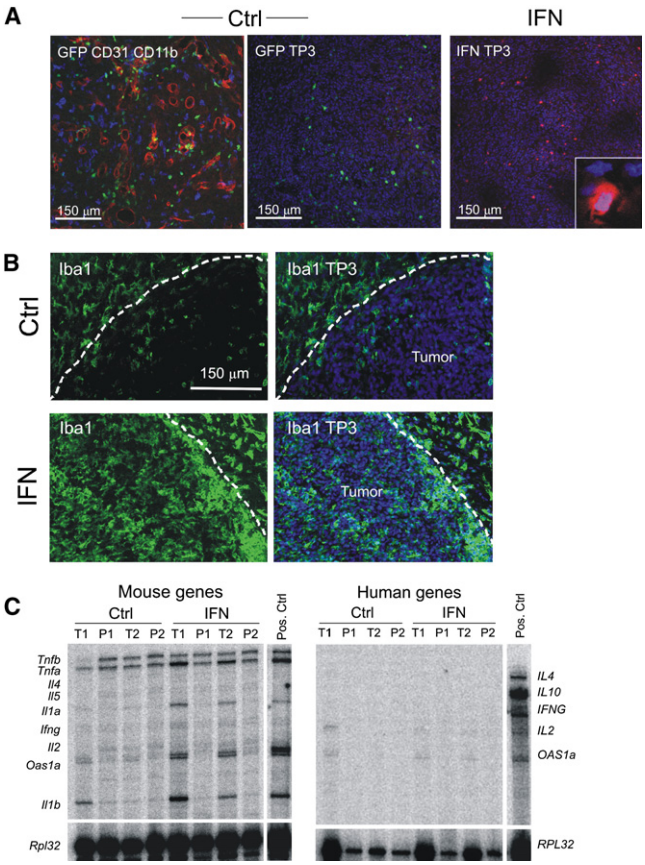

Figure 3. Tumor-Targeted IFN Response in Tie2-IFN Athymic Mice

(A and B) GFP or Iba1 immunostaining (green), CD31 or IFN-α immunostaining (red), and CD11b immunostaining or TP3 nuclear staining (blue) of intracranial gliomas grown in control Tie2-GFP (Ctrl) and Tie2-IFN (IFN) mice. Inset in (A) shows high-power magnification of an IFN-α-expressing cell. Brain sections were analyzed at 4 or 5 weeks PTI. Photos are representative of results obtained from 3–6 mice per group.

(C) RNase protection assay performed at 4 weeks PTI using mouse (left panel) or human (right panel) gene probes. T, tumor; P, brain parenchyma from contralateral hemisphere. The housekeeping gene *RPL32* was used to estimate the amount of mouse and human mRNA in each sample. The rightmost lane in each panel represents positive control. Results are representative of 4 Tie2-IFN (IFN) and 4 PGK-GFP (Ctrl) mice analyzed at 4 (n = 2) or 5 (n = 2) weeks PTI.

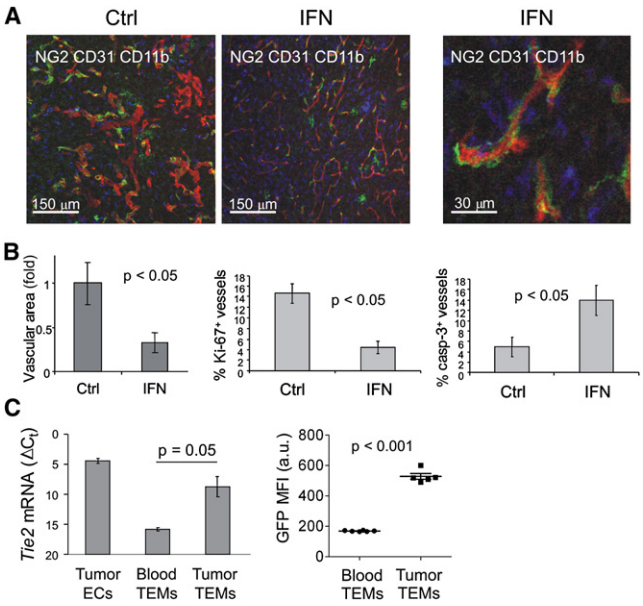

Figure 4. Inhibition of Glioma Angiogenesis in Tie2-IFN Mice and Preferential Activation of the *Tie2* Promoter/Enhancer in the Tumor Microenvironment

(A) NG2 (green), CD31 (red), and CD11b (blue) immunostaining of intracranial gliomas grown in control Tie2-GFP (Ctrl) and Tie2-IFN (IFN) mice. The rightmost panel shows high-power magnification of a tumor vessel covered by NG2$^+$ pericytes. Brain sections were analyzed at 4 or 5 weeks PTI. Photos are representative of results obtained from 3–6 mice per group.

(B) Vascular area (mean fold increase over reference value [Ctrl] ± SD) and quantification of Ki-67$^+$CD31$^+$ or caspase-3$^+$CD31$^+$ ECs (mean frequency of marker-positive cells, % ± SD) in gliomas of control (Ctrl, includes Tie2-GFP [n = 5] and PGK-GFP [n = 3]) and Tie2-IFN (IFN; n = 5) mice. Brain sections were analyzed at 4 or 5 weeks PTI.

(C) Left: qPCR analysis of *Tie2* transcript in tumor-derived ECs and Tie2-expressing monocytes (TEMs) and blood-derived TEMs isolated from FVB/Tie2-GFP transgenic mice. Results show ΔC_t values (mean ± SEM; n = 2 biological samples) versus endogenous control *Gapdh*. The lower the ΔC_t, the higher the expression of the transcript. Tumor-derived ECs are used as a reference Tie2$^+$ cell type. Right: GFP MFI (in mean arbitrary units [a.u.] ± SEM; n = 5–6) of blood- and tumor-derived TEMs from Tie2-GFP transgenic mice.

We measured the expression of endogenous *Tie2* mRNA by quantitative PCR (qPCR) in TEMs isolated to near homogeneity from FVB/Tie2-GFP transgenic mice (De Palma et al., 2005b) carrying subcutaneous N202 breast carcinomas. We found that *Tie2* mRNA was expressed more in tumor-derived than in blood-derived TEMs (Figure 4C). Similarly, when we measured the expression of the *Tie2* promoter/enhancer-driven GFP transgene, we found that the GFP MFI was higher (~3-fold) in tumor- versus blood-derived TEMs (Figure 4C). These findings suggest that promoter-dependent upregulation of transgene expression at the tumor site, together with the preferential homing of TEMs to angiogenic blood vessels, contributes to effectively targeting IFN-α to tumors.

Inhibition of Established Mammary Tumors in MMTV-PyMT Transgenic Mice

We then assayed the antitumor activity of IFN-α in a spontaneous model of mammary carcinogenesis. In the MMTV-PyMT mouse model (FVB strain), multiple breast tumors caused by expression of the polyoma middle T (PyMT) oncoprotein in the mammary epithelium progress through well-characterized stages, and 90% of the tumor-bearing mice develop lung metastases by 12–14 weeks of age (Husemann et al., 2008; Lin et al., 2001, 2003).

We studied the recruitment of TEMs to MMTV-PyMT tumors. We transplanted HSPCs obtained from Tie2-GFP transgenic mice (De Palma et al., 2005b) into 5.5-week-old female MMTV-PyMT mice (Figure 5A), which are known to carry mammary lesions developed to the hyperplastic/dysplastic stage (Husemann et al., 2008; Lin et al., 2001, 2003). We then analyzed the tumors 1.5, 4, and 6 weeks later (i.e., at 7, 9.5, and 11.5 weeks of age, respectively). Examination of the mammary glands of the transplanted mice revealed the presence of multiple

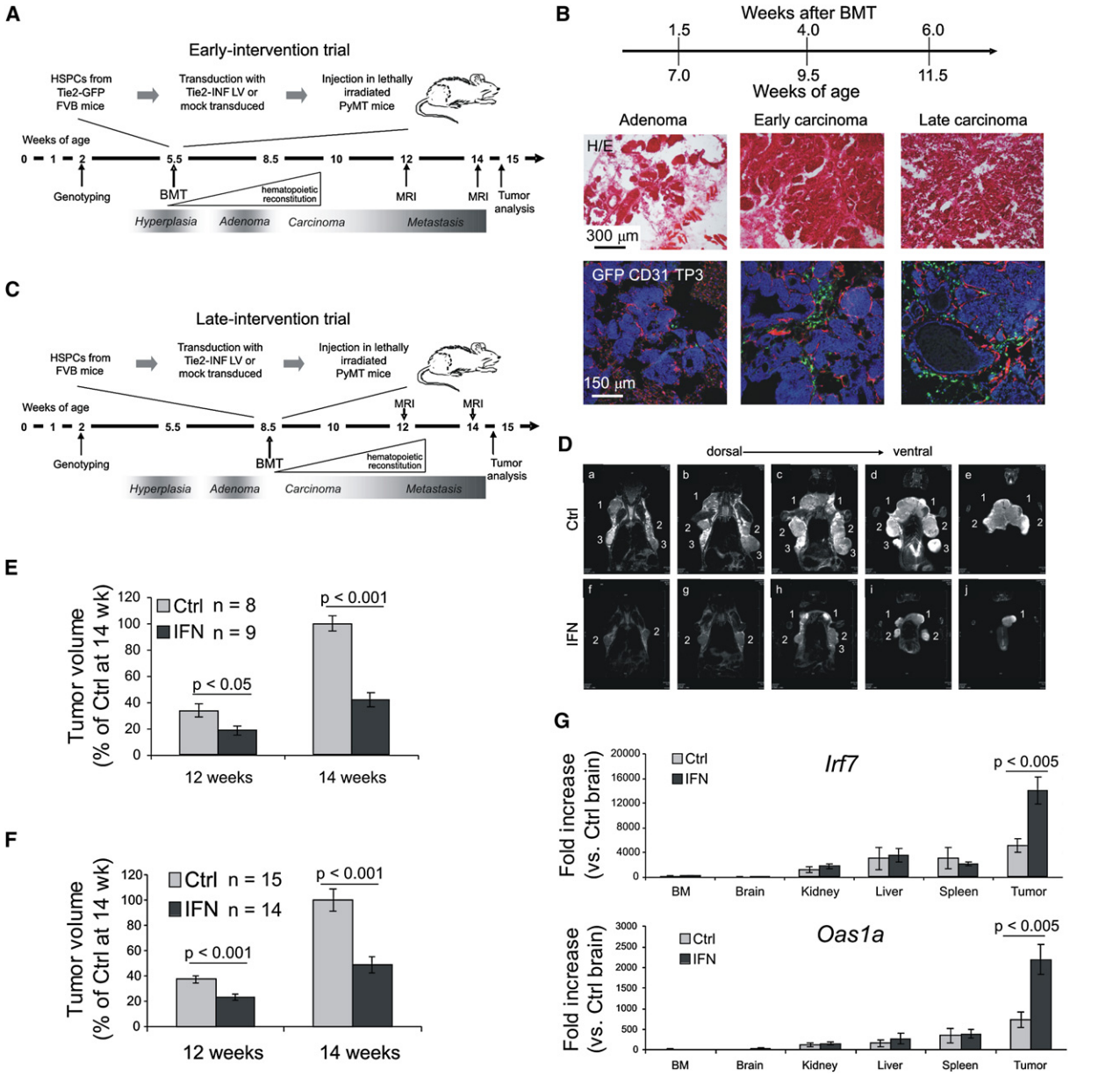

Figure 5. Inhibition of Established Mammary Tumors in Tie2-IFN MMTV-PyMT Mice

(A) Schematic of the early-intervention trial.

(B) Representative sections of breast tumors (n = 2 mice per group; 5–12 tumors per mouse) analyzed 1.5, 4, and 6 weeks after transplantation of Tie2-GFP-transgenic HSPCs into 5.5-week-old MMTV-PyMT mice. Top row of images: H&E staining. Bottom row of images: GFP (green) and CD31 (red) immunostaining and TP3 nuclear staining (blue).

(C) Schematic of the late-intervention trial.

(D) Tumor growth in representative mice treated according to an early-intervention schedule. Axial noncontiguous serial T2-weighted MRI images (a–e and f–j) show primary tumors at the three anterior mammary glands (1, 2, and 3) of representative control (Ctrl; a–e) and Tie2-IFN (IFN; f–j) MMTV-PyMT mice at 14 weeks of age.

(E) Mammary tumor growth (mean volume ± SEM by MRI analysis of the three anterior mammary glands) at 12 and 14 weeks of age in control (Ctrl; n = 8) and Tie2-IFN (IFN; n = 9) MMTV-PyMT mice treated according to an early-intervention schedule (two experiments combined).

(F) Mammary tumor growth (mean volume ± SEM) at 12 and 14 weeks of age in control (Ctrl; n = 15) and Tie2-IFN (IFN; n = 14) MMTV-PyMT mice treated according to a late-intervention schedule (two experiments combined).

(G) *Irf7* (top) and *Oas1a* (bottom) expression as measured by qPCR (mean fold increase over reference value [control brain] ± SEM) in tumors and organs of control (Ctrl; n = 4 for organs; n = 8 for tumors) and Tie2-IFN (IFN; n = 4 for organs; n = 9 for tumors) MMTV-PyMT mice. Samples were analyzed at 14.5 weeks of age. Only p values < 0.05 are indicated.

hyperplastic/dysplastic lesions at 7 weeks of age, whereas early and locally invasive carcinomas were observed at 9.5 and 11.5 weeks (Figure 5B). We detected GFP$^+$ TEMs in the tumors at 4 and 6 weeks (carcinoma stage), but not at 1.5 weeks (hyperplasia/adenoma stage) posttransplant (Figure 5B). These findings suggest that TEM-mediated gene delivery at the tumor site is delayed a few weeks following HSPC transplantation. This is consistent with both the expected kinetics of hematopoietic reconstitution from the transplanted HSPCs and the enhanced recruitment of BM-derived myeloid cells that occurs concomitantly with malignant transition (de Visser et al., 2006; Lin et al., 2001).

We then transplanted Tie2-IFN LV-transduced or mock-transduced HSPCs into either 5.5- or 8.5-week-old female MMTV-PyMT mice. Because of the delayed TEM recruitment to the tumors, both gene delivery schedules target established carcinomas and can be regarded as "early" and "late" intervention trials, respectively (Figures 5A and 5C). We observed a clear delay in the onset and development of mammary tumors in Tie2-IFN- (IFN) versus mock-transduced (Ctrl) mice in two independent early-intervention trials as assessed by biweekly inspections of the mammary glands (data not shown). Further analyses performed by MRI showed that tumor growth was significantly inhibited in Tie2-IFN mice (Figures 5D and 5E): at 12 weeks of age, tumor volume in Tie2-IFN mice (n = 9) was 56% of that of control mice (n = 8), and this difference increased at 14 weeks of age, when tumor volume in Tie2-IFN mice was only 42% of that of the controls. When we transplanted MMTV-PyMT mice according to a late-intervention schedule (8.5 weeks of age), tumors were already palpable in the majority of mammary glands. We obtained significant inhibition of tumor growth in two independent experiments (Figure 5F): at 12 weeks of age, the tumor volume in Tie2-IFN mice (n = 14) was 62% of that of control mice (n = 15), and this difference increased at 14 weeks of age, when the tumor volume in Tie2-IFN mice was only 49% of that of control mice. Together, these data show significant antitumor responses both in early- and late-intervention trials and demonstrate the increasing therapeutic activity at 14 versus 12 weeks. It is noteworthy that these IFN responses were achieved in spite of the relatively low vector copy number per cell in the BM of the transplanted mice examined at the end of the experiments (Tie2-IFN 0.35 ± 0.09; n = 13). In these experiments, MRI data were confirmed by postmortem tumor weight measurements performed at 14.5 weeks (data not shown), when all of the mice were euthanized because of the large tumor burden in control mice.

We then investigated the antitumor responses in Tie2-IFN mice. To prove that tumor inhibition was associated with in situ activation of a type I IFN response, we measured the expression of the interferon-inducible genes interferon regulatory factor-7 (*Irf7*) and *Oas1a* at 14.5 weeks of age (Honda et al., 2005; Stark et al., 1998) by qPCR in tumors and organs of the transplanted mice. Both genes were significantly upregulated in tumors of Tie2-IFN mice as compared to those in controls (Figure 5G). By contrast, we found no increase of *Irf7* and *Oas1a* in the organs of Tie2-IFN mice. This was also true for BM, spleen, and liver, which contain substantial hematopoietic populations derived from the transplanted HSPCs. These data provide molecular evidence for the selective targeting of the IFN response to the tumors of Tie2-IFN MMTV-PyMT mice.

Tumor-infiltrating hematopoietic cells are important effectors of tumor rejection processes (Willimsky and Blankenstein, 2007). Whereas the frequency of infiltrating CD45$^+$ hematopoietic cells and CD68$^+$ macrophages was similar in Tie2-IFN and control tumors, there was a dramatic increase in the fraction of innate immune cells expressing DC (CD11c) and cell activation markers (Iba1) specifically in Tie2-IFN tumors (Figure 6A and data not shown). Of note, a substantial proportion of the CD11c$^+$ DCs and CD68$^+$ macrophages coexpressed Iba1 in Tie2-IFN tumors, a feature consistent with IFN-mediated activation (Tosi et al., 2004). NK cells, identified by expression of the alpha 2 integrin (CD49b/DX5), were observed at low frequency in both Tie2-IFN and control tumors and were mostly found clustered in discrete tumor areas (Figure S3). When isolated from the spleen of tumor-bearing mice, NK cells of Tie2-IFN mice had superior cytolytic activity as compared to cells from control mice (Figure 6B). Regarding adaptive immune cells, we found greatly increased infiltration of both CD4$^+$ and CD8$^+$ T lymphocytes in Tie2-IFN tumors as compared to controls (Figure 6C). These findings were confirmed by fluorescence-activated cell sorting (FACS) analysis of tumor-derived single-cell suspensions (Figure 6D). Importantly, the frequency of effector T cells (Openshaw et al., 1995) was higher in Tie2-IFN tumors than in control tumors as revealed by expression of CD44 in CD4$^+$ and CD8$^+$ T cells and their ability to express IFN-γ upon restimulation ex vivo. Together, these findings suggest that TEM-mediated IFN-α delivery enhances the recruitment and promotes the activation of both innate and adaptive immune cells.

We noted that tumor growth in MMTV-PyMT mice was associated with a progressive increase in blood leukocyte counts and a measurable decrease in erythrocyte counts and hemoglobin level (Figure 7A). IFN-α delivery by TEMs attenuated such tumor-driven hematological abnormalities (Figure 7B); importantly, these effects could not be interpreted as IFN-induced toxicity because the number of circulating platelets and the frequency of BM-derived colony-forming cells (CFCs) were similar in Tie2-IFN, control (transplanted), and wild-type (nontransplanted) mice (Figures 7B and 7C). In transplanted tumor-bearing mice, the majority of the circulating leukocytes were CD11b$^+$ or CD11b$^+$Gr1$^+$ myeloid cells (Figure S4), which have been shown to be protumoral and proangiogenic (Shojaei et al., 2008). Of note, the CD11b$^+$ myeloid cell counts were significantly reduced in the IFN-treated mice (Figure S4).

We observed TEMs at the expected frequency in both blood and tumors of Tie2-IFN and control mice (Figure 7D; Figure S4), indicating that the expression of the *Ifn1a* transgene does not affect TEM mobilization from the BM, nor does it impair their homing to tumors.

Suppression of Metastasis in MMTV-PyMT Transgenic Mice

We then analyzed the lungs of MMTV-PyMT mice treated according to an early-intervention schedule to detect antitumor responses at the metastatic site. We analyzed the lungs of transplanted mice by serial sectioning the entire left lung and scoring for the presence of metastatic nodules (Figures 8A and 8B). All control mice had metastatic outgrowth in the lung, with 7 of 8

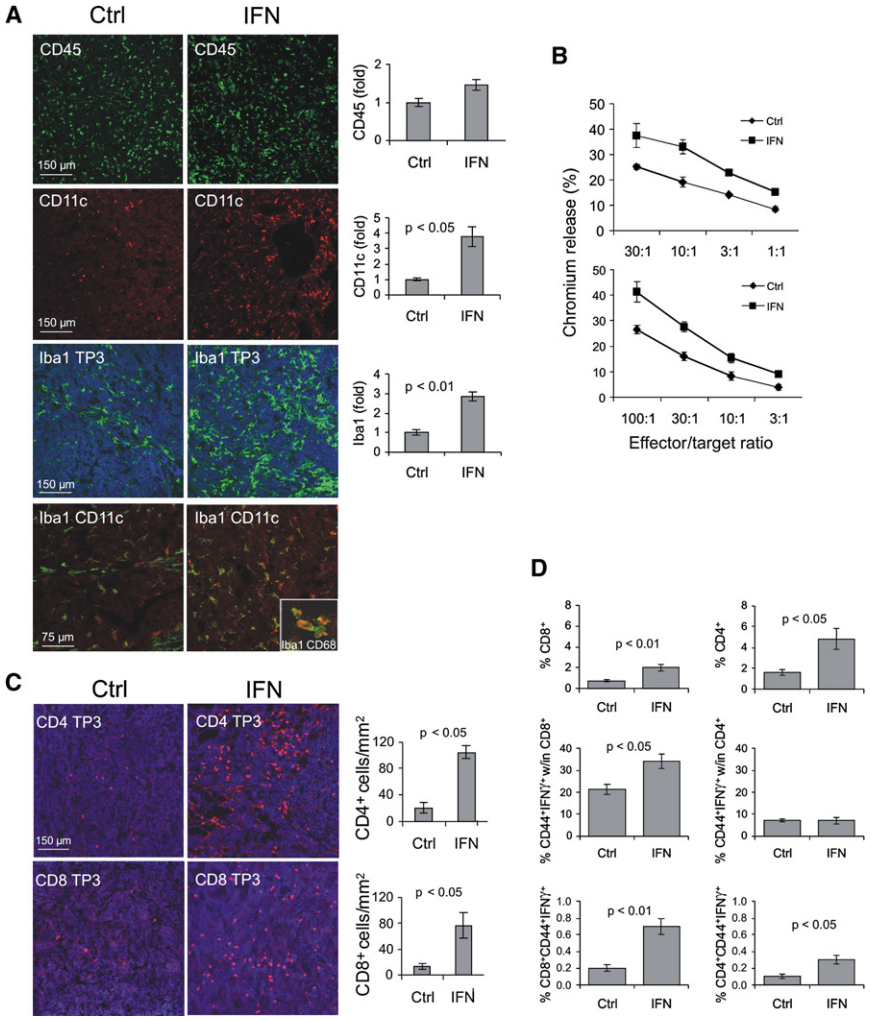

Figure 6. Immune Cell Activation in Tie2-IFN MMTV-PyMT Mice

(A) CD45 or Iba1 (green) and CD11c or CD68 (red) immunostaining and TP3 nuclear staining (blue) of MMTV-PyMT mammary tumors grown in control (Ctrl) and Tie2-IFN (IFN) mice. Tumors were analyzed at 14.5 weeks of age. Histograms at right show quantification of CD45$^+$, Iba1$^+$, and CD11c$^+$ areas (mean fold increase over reference value [Ctrl] ± SEM; n = 3 mice per group; n = 12 tumors per mouse).

(B) NK chromium release assays. Cytolytic activity at different effector (NK cells)/target (YAC-1 cells) ratios of NK cells obtained from the spleen of control (Ctrl) and Tie2-IFN (IFN) tumor-bearing mice (percentage of maximal chromium release ± SEM; n = 3–5 technical replicates) is shown. Two independent experiments are shown. $p \leq 0.01$ at all effector/target ratios.

(C) CD4 or CD8 immunostaining (red) and TP3 nuclear staining (blue) of MMTV-PyMT mammary tumors grown in control (Ctrl) and Tie2-IFN (IFN) mice. Tumors were analyzed at 14.5 weeks of age. Histograms at right show quantification of CD4$^+$ and CD8$^+$ cells (mean frequency of marker-positive cells, % ± SEM; n = 3 mice per group; n = 4 tumors per mouse).

(D) FACS analysis of tumor-derived cells (mean frequency of marker-positive cells, % ± SEM; n = 7 mice per group; n = 5 tumors per mouse). Upper histograms: frequency of CD8$^+$ or CD4$^+$ cells after physical gating on viable tumor-derived cells. Middle histograms: frequency of CD44$^+$IFN-γ$^+$ cells within CD8$^+$ or CD4$^+$ cells. Lower histograms: frequency of CD8$^+$CD44$^+$IFN-γ$^+$ or CD4$^+$CD44$^+$ IFN-γ$^+$ effector T cells within viable tumor-derived cells. Before analysis of IFN-γ expression, cells were stimulated ex vivo by phorbol myristate acetate (PMA) and ionomycin.

mice showing metastatic foci in virtually all examined lung sections, indicating that multiple and large metastases had developed in these mice (0.4–25.2 metastatic foci per section per mouse, average 9.2; n = 8 mice; 16–24 sections examined per mouse). By contrast, Tie2-IFN mice were either free from detectable nodules (n = 3) or had few small foci per lung (0–0.8 metastatic foci per section per mouse, average 0.2; n = 9 mice; 16–24 sections examined per mouse; $p < 0.001$ for control versus Tie2-IFN by Mann-Whitney test). When we calculated the total tumor area in the examined lung sections of each mouse, it was ~300-fold higher in control versus Tie2-IFN mice ($p < 0.001$ by Mann-Whitney test). These results indicate that our therapeutic strategy can effectively suppress metastasis in MMTV-PyMT mice.

Wound Healing in Tie2-IFN Mice

Our studies demonstrated that TEM-mediated IFN-α delivery achieved substantial antitumor activity without causing detectable hematopoietic toxicity. We then investigated whether this strategy would impair tissue repair. To address this question, we performed a wound healing assay in FVB/Tie2-IFN and control mice 8 weeks after HSPC transplantation. We found no evidence of impaired wound healing in Tie2-IFN mice as assessed by monitoring the healing response (Figure 8C) and by histological examination of the skin at 10 days post injury (Figure 8D). As shown in Figure 8D, keratinocyte proliferation and angiogenesis were induced similarly below the wound in both control and Tie2-IFN mice.

DISCUSSION

Monocyte-Mediated Targeting of IFN-α to Tumors

Here, we describe a gene delivery strategy to target IFN-α to tumors. By exploiting LV gene transfer into HSPCs and making transgene expression responsive to the signals that activate *Tie2* in tumor-infiltrating hematopoietic cells, we turned proangiogenic monocytes into efficient cellular vehicles for the targeted delivery of IFN-α to tumors. In orthotopic human gliomas and transgenic mice spontaneously developing metastatic breast cancer, IFN-α-expressing TEMs triggered antitumor responses in the absence of systemic IFN-α expression, and without inducing detectable toxicity. In these mice, antitumor responses recapitulated the well-known activities of type I IFNs: inhibition of angiogenesis, recruitment and activation of innate and adaptive immune cells, and induction of cell apoptosis.

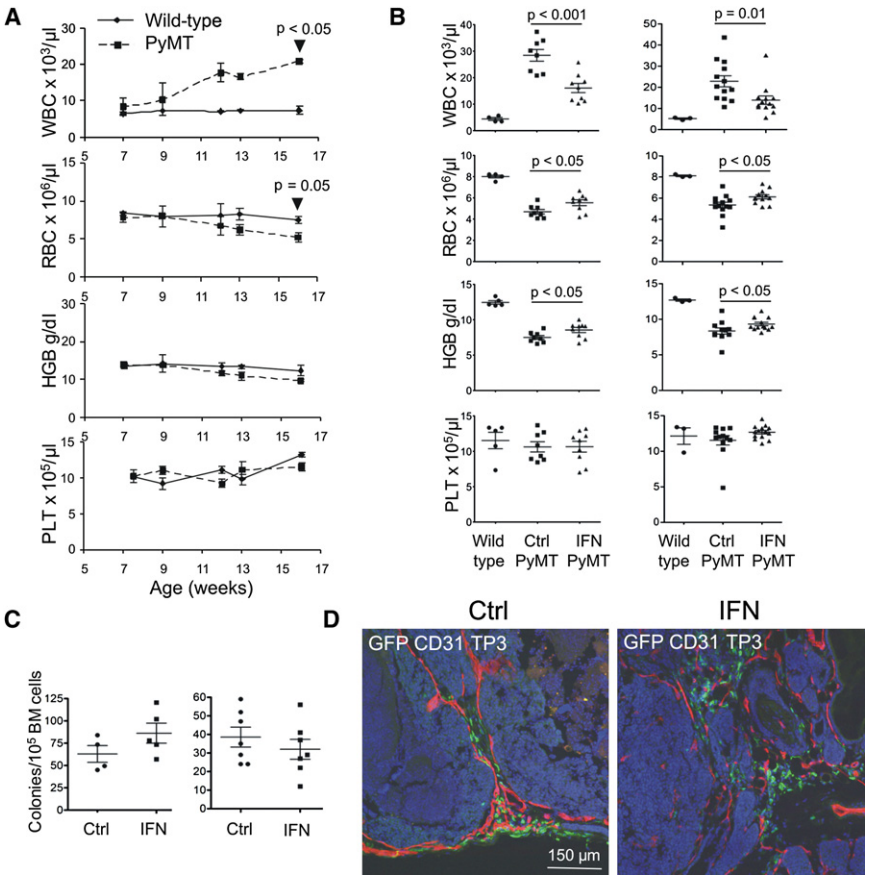

Figure 7. Lack of Myelotoxicity in Tie2-IFN MMTV-PyMT Mice

(A) Blood cell counts and hematological parameters (mean values ± SEM) of nontransplanted FVB (wild-type; n = 3) and MMTV-PyMT (PyMT; n = 3) mice analyzed at the indicated time points. Abbreviations as in Figure 1E.

(B) Blood cell counts and hematological parameters (mean values ± SEM) of mice from early (left panels) and late (right panels) intervention trials. Data from individual nontransplanted FVB (wild-type; n = 3–5) and transplanted control (Ctrl; n = 9–13) and Tie2-IFN (IFN; n = 9–13) MMTV-PyMT mice are shown. Analyses were performed at 14.5 weeks of age.

(C) Colony-forming cell (CFC) assays (mean number of CFCs/10^5 BM cells ± SEM) in BM of control (Ctrl; n = 4–7) and Tie2-IFN (IFN; n = 5–7) MMTV-PyMT mice, as measured at 14.5 weeks of age. Two independent experiments (left, early-intervention trial; right, late-intervention trial) are shown. $p > 0.05$ for both experiments.

(D) GFP (green) and CD31 (red) immunostaining and TP3 nuclear staining (blue) of representative control (Ctrl) and Tie2-IFN (IFN) MMTV-PyMT tumors analyzed at 14.5 weeks of age (n = 4).

IFN-α has been used for the treatment of several types of cancer, including hematological malignancies, melanoma, Kaposi's sarcoma, and renal carcinoma (Belardelli et al., 2002; Brassard et al., 2002). However, only a small proportion of patients benefit from IFN therapy, and significant toxicity is often associated with the maximal tolerated doses that are required to obtain therapeutic responses. Several factors may limit the efficacy of systemic IFN therapy. First, IFN bioavailability at the tumor site may vary significantly with the tumor type, burden, and administration protocol. Intravenous and subcutaneous dosing of recombinant type I IFN are associated with a systemic half-life of a few hours, which may expose the tumor to only short bursts of therapy (Salmon et al., 1996). In addition, preclinical studies in mouse models have indicated that antitumor activity of IFNs displays a bell-shaped dose-response curve (Slaton et al., 1999; Solorzano et al., 2003). These data suggest that maximal tolerated doses may induce counterregulatory mechanisms that disable cytokine activity, whereas optimal biological doses may be therapeutic (Curnis et al., 2005; Shaked et al., 2005). Yet it may be difficult to identify optimal biological doses in cancer patients, and clinical testing of low-dose IFN-α showed no impact on survival in melanoma patients (Belardelli et al., 2002). Thus, delivery strategies that target type I IFNs to the tumor site without inducing systemic overexpression may be advantageous.

The bone marrow is a source of nonendothelial, proangiogenic hematopoietic cells that are recruited to tumors, where they appear to provide paracrine support for angiogenesis (De Palma et al., 2003; De Palma and Naldini, 2006; Ahn and Brown, 2008). By using tumor-infiltrating monocytes as a cellular vehicle for the transport of IFN-α to tumors, we speculated that continuous, low-dose IFN-α would be released at the tumor site, possibly achieving biologically active concentrations without inducing counterregulatory responses and systemic toxicity. We observed strong antitumor responses in Tie2-IFN mice in spite of the fact that IFN-α was not detectable in the plasma by ELISA and demonstrated in situ activation of type I IFN signaling in tumors. TEMs effectively and selectively targeted IFN to the tumors, as shown by the upregulation of IFN-inducible genes in the tumors but not in the other tissues and organs analyzed. The tumor-homing specificity of TEMs, together with the upregulation of the *Tie2* promoter/enhancer-driven transgene in TEMs upon their homing to the tumor, may well explain the selectivity of IFN-α expression at the tumor site, the effective antitumor activity, and the lack of myelotoxicity in Tie2-IFN mice. It is possible that IFN-α, when released by TEMs in the tumor microenvironment, may induce expression of endogenous IFN genes in neighboring cells through a paracrine loop, in analogy with spreading antiviral responses triggered by type I IFNs (Stetson and Medzhitov, 2006). In this regard, the sensitivity of the immunostaining procedure used to detect IFN-α-producing TEMs in our studies may have prevented the detection of a larger fraction of tumor-associated cells expressing IFN-α at low level.

Mechanisms of Antitumor Activity: Inhibition of Angiogenesis and Activation of Immune Cells

Concerning the mechanisms of antitumor activity, we noted a clear antiangiogenic effect in human gliomas inoculated in

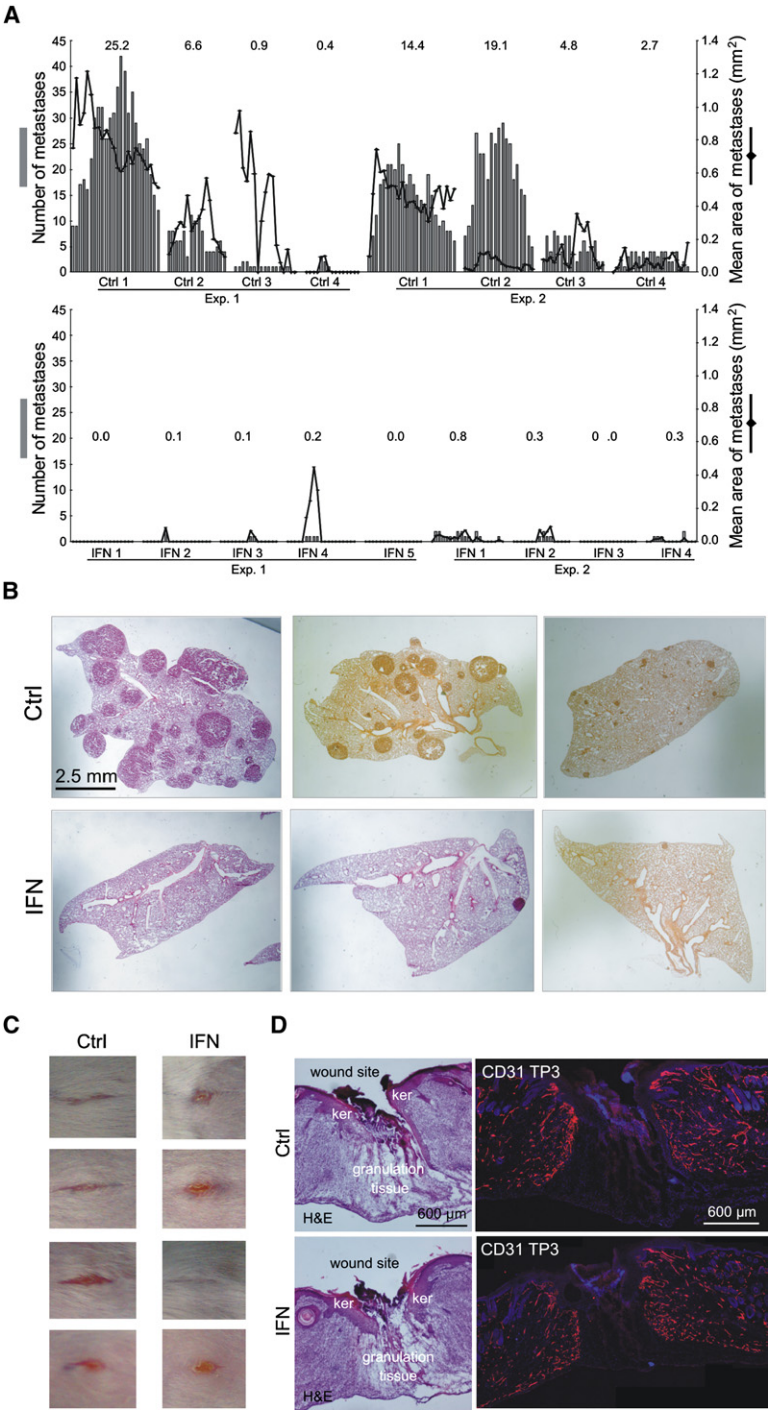

Figure 8. Inhibition of Metastasis and Normal Wound Healing in Tie2-IFN MMTV-PyMT Mice

(A) Number of metastatic foci (gray bars) and mean area of single metastasis (broken black line) in individual serial sections (individual bars) obtained from the entire left lung of individual control (Ctrl; n = 8) and Tie2-IFN (IFN; n = 9) MMTV-PyMT mice treated according to an early-intervention schedule and analyzed at 14.5 weeks of age. Numbers indicate the average number of metastases per section in each individual mouse. See text for statistical analysis.

(B) H&E staining of representative lung sections of control (Ctrl; n = 8) and Tie2-IFN (IFN; n = 9) MMTV-PyMT mice analyzed at 14.5 weeks of age.

(C) Photos of healing of wounds at 10 days post injury in control (Ctrl; n = 4) and Tie2-IFN (IFN; n = 4) FVB mice.

(D) Left panels: H&E staining of representative (n = 4) skin sections analyzed at 10 days post injury. ker: keratinocytes. Right panels: CD31 immunostaining (red) and TP3 nuclear staining (blue) of adjacent sections. Wide-field images showing CD31 immunostaining were reconstructed by superimposition of overlapping confocal planes acquired at 100× magnification.

Tie2-IFN mice. In these tumors, the relative vascular area was greatly reduced and the blood vessels had features of co-opted or ''normalized'' vasculature, consistent with the reported angiostatic activities of type I IFNs. The preferential localization of TEMs in the proximity of sprouting blood vessels may contribute to this antiangiogenic effect, by generating locally effective IFN-α concentration at the angiogenic site. Type I IFNs can inhibit angiogenesis by exerting direct antiproliferative and proapoptotic activity on ECs and by downregulating the expression of proangiogenic factors in tumor cells (Dinney et al., 1998; Slaton et al., 1999; Solorzano et al., 2003). We did not observe an antiangiogenic effect in the mammary tumors of Tie2-IFN mice (data not shown), suggesting the prevalence of other mechanisms driving the antitumor response in this model.

Activation of tumor-infiltrating immune cells may represent one such mechanism. Indeed, we observed robust upregulation of Iba1, a macrophage-lineage activation marker, in tumor-associated macrophages and DCs of Tie2-IFN mice. In the MMTV-PyMT model, we found enhanced tumor infiltration by DCs and effector T cells and activation of NK cells. The finding of activated NK cells in the spleen of Tie2-IFN mice may seem to contradict the notion that TEM-mediated IFN responses are specifically targeted to tumors. However, it has been shown that DCs activated by type I IFNs migrate to lymphoid organs, where they are able to transactivate NK cells via the release of IL-15 (Lucas et al., 2007). We observed greatly enhanced infiltration of Iba1$^+$CD11c$^+$ DCs in the tumors of Tie2-IFN MMTV-PyMT mice, consistent with the ability of IFN-α to promote DC maturation and activation (Belardelli et al., 2002; Brassard et al., 2002; Tosi et al., 2004). It can be envisioned that IFN-activated DCs may in turn activate NK cells in the lymphoid organs of Tie2-IFN mice. Of note, the enhanced recruitment and activation of DCs in the tumors of IFN-treated mice may also contribute to promote antitumor immunity by other immune cell types, such as T cells. Because wound healing was not impaired in Tie2-IFN mice, it is likely that the induction of immune responses has a key role in mediating the antitumor activity of IFN-α.

Schreiber and colleagues have shown that host hematopoietic cells, and not tumor cells, need to express functional type I IFN receptor (IFNAR)—and thus be sensitive to type I IFNs—for tumor rejection to occur (Dunn et al., 2006). In another study, the

antitumor activity of exogenously administered IFN-α was abrogated in Stat1-deficient hosts, which are insensitive to IFN-α (Lesinski et al., 2003). These data indicate that both endogenous and exogenous type I IFNs primarily target tumor-infiltrating/stromal cells. Perhaps our most relevant finding in support of this notion was obtained in the glioma model. Indeed, in tumors of these mice, IFN-inducible genes were strongly upregulated in the host compartment, but not in the tumor cells, which are of human origin and insensitive to mouse IFN-α. Yet the IFN response targeted to the host-derived components of the tumor was sufficient to inhibit tumor growth. From a clinical perspective, a therapeutic strategy targeting the tumor stroma may be applied to a broad range of tumors and may have a lower likelihood to select resistance. Moreover, therapeutic responses may also be obtained in the absence of an adaptive immunity against tumor-associated antigens.

Effects on Metastasis

A remarkable result was the near complete control of metastatic growth obtained in MMTV-PyMT Tie2-IFN mice treated according to an early-intervention schedule. Because metastatic dissemination occurs early in this breast cancer model (Husemann et al., 2008), it is unlikely that the reduced primary tumor burden in Tie2-IFN mice fully accounts for the suppression of metastasis. Rather, we can envisage that the cytostatic and cytotoxic responses triggered by IFN at the primary tumor site may have prevented progression to a metastatic stage (Kouros-Mehr et al., 2008). In the late-intervention trial, we achieved significant control of the primary tumors but could not reliably assess efficacy on metastases. Indeed, we found many fewer and smaller metastases, in both control and treated mice, than in early-intervention trials, possibly as a consequence of the late irradiation schedule (data not shown). In addition, it is likely that the short follow-up time available in the late-intervention trial would not allow for detecting a significant response at the metastatic site. Future studies in other metastatic tumor models that allow for longer follow-up times will be needed to ascertain the therapeutic potential of TEM-mediated IFN delivery on established metastases.

Clinical Relevance and Therapeutic Opportunities

Our results indicate that full donor chimerism with gene-modified cells in transplanted mice is not required to achieve therapeutic benefit. Indeed, transplanted mice carried an average of 0.4–0.6 Tie2-IFN LV copies per cell at long-term analysis, with some mice showing as few as 0.1 copies per cell. These data argue in favor of the feasibility of a future clinical translation of our strategy. Indeed, one could perform minitransplant of gene-modified autologous HSPCs based on mild conditioning or infuse gene-modified HSPCs together with unmodified cells, in combination with or subsequent to standard cancer therapies. On the basis of available data, high-dose chemotherapy followed by autologous HSPC transplantation can be regarded as a clinical option not only for several hematologic malignancies but also for certain types of solid cancers, including neuroblastoma, Ewing sarcoma, and germ cell tumors (Ljungman et al., 2006). Our mouse glioma model may suggest that transplantation of gene-modified autologous HSPCs could prevent or delay the local recurrence of glioblastoma in cancer patients following surgical debulking or irradiation of the tumor mass. Our data from MMTV-PyMT mice treated according to a late-intervention schedule further suggest that antitumor responses might be obtained even in patients with advanced and metastatic cancer. Although we did not observe obvious myelotoxicity when we delivered IFN-α by TEMs, Tie2 is expressed by primitive hematopoietic stem cells (Jones et al., 2001). Thus, further long-term studies, also employing human hematochimeric mouse models, should be performed to better assess the potential toxicity of our delivery strategy. If required, advanced-design LVs may be developed to restrict IFN-α expression to mature hematopoietic cells (Brown et al., 2006) or to the desired time window (Vigna et al., 2005), and the inclusion of a suicide gene in the gene expression cassette may enable elimination of the gene-modified cells if required (Bordignon, 2006).

Because of their reported tumor tropism, distinct types of stem cells—including mesenchymal and neural stem cells—are currently being tested as gene delivery vehicles for cell-based cancer therapy (Aboody et al., 2008). However, these cell types must be exogenously infused in large amounts, and their inherent protumoral or immunosuppressive activities might represent a threat to successful therapy. Our gene delivery strategy is not based on additive cell therapy; rather, it exploits an endogenous cell compartment, which is renewed constantly by long-term repopulating cells. Moreover, by turning TEMs into IFN-expressing cells, our strategy antagonizes the protumoral activity of a naturally occurring tumor-infiltrating cell type.

Tumor-associated hematopoietic cells have long been thought to represent ideal vehicles for the transport of therapy to tumors (Bordignon, 2006). However, this strategy has been hampered until now by inefficient gene delivery into long-term repopulating cells and the lack of a suitable cellular vehicle that could be used to safely and selectively transfer the therapeutic factor to tumors. Our studies now provide proof of feasibility of a gene therapy strategy wherein ex vivo transduction of HSPCs can be used to safely and effectively deliver IFN-α, and possibly other cancer biotherapeutics, in a tumor-targeted fashion.

EXPERIMENTAL PROCEDURES

Lentiviral Vectors

The Tie2-GFP and PGK-GFP lentiviral transfer vectors were described previously (De Palma et al., 2005b). The Tie2-IFN and PGK-IFN lentiviral transfer vectors were generated by cloning a murine *Ifna1* cDNA in place of the GFP cDNA into the Tie2-GFP and PGK-GFP lentiviral transfer vectors, respectively. Concentrated VSV-G-pseudotyped LV stocks were produced and titered as described previously (De Palma and Naldini, 2002).

Mice

FVB and CD1 athymic (*nu/nu*) mice were purchased from Charles River Laboratories (Calco, Milan). FVB/MMTV-PyMT mice were purchased from the NCI-Frederick Mouse Repository and established as a colony at the San Raffaele animal facility. The strain was maintained by breeding hemizygous males with FVB wild-type females. FVB/Tie2-GFP transgenic mice were generated by LV-mediated transgenesis as described previously (De Palma et al., 2005b). All procedures were performed according to protocols approved by the Animal Care and Use Committee of the Fondazione San Raffaele del Monte Tabor (IACUC 231, 324, 335) and communicated to the Ministry of Health and local authorities according to Italian law.

HSPC Transduction and Transplantation

Six-week-old female CD1 athymic, FVB, and FVB/Tie2-GFP mice were killed with CO_2, and BM was harvested by flushing the femurs and tibias.

Lineage-negative cells enriched in HSPCs were isolated from BM using a cell purification kit (StemCell Technologies) and transduced with concentrated LVs as described previously (De Palma and Naldini, 2002; De Palma et al., 2003). Briefly, 10^6 cells/ml were transduced with a LV dose equivalent to 3–4 μg/ml HIV p24 (for Tie2-IFN and PGK-IFN LVs) or 10^8 GFP-transducing units/ml (for Tie2-GFP and PGK-GFP LVs) for 12 hr in serum-free StemSpan medium (StemCell Technologies) containing a cocktail of cytokines (10 ng/ml IL-3, 20 ng/ml IL-6, 100 ng/ml SCF, and 10 ng/ml FL-3L, all from Serotec). After transduction, 10^6 cells were infused into the tail vein of lethally irradiated 6-week-old female CD1 athymic or 5.5- or 8.5-week-old FVB/MMTV-PyMT mice (radiation doses were 975 cGy for CD1 mice and 1100 cGy for FVB mice). Transduced cells were also cultured in vitro for 5 days before FACS analysis or for 9 days to measure IFN-α secretion by ELISA (R&D Systems). Vector copy number in BM cells was measured by qPCR of vector sequences at the end of the experiments as described previously (De Palma et al., 2005a). Colony-forming cell assays were performed as described previously (De Palma and Naldini, 2002; De Palma et al., 2003).

Statistical Analysis

In all studies, values are expressed as mean ± standard deviation (SD) or standard error of the mean (SEM), as indicated. Statistical analyses were performed by unpaired Student's t test unless indicated otherwise. Differences were considered statistically significant at $p < 0.05$.

SUPPLEMENTAL DATA

The Supplemental Data include Supplemental Experimental Procedures, Supplemental References, and four figures and can be found with this article online at http://www.cancercell.org/cgi/content/full/14/4/299/DC1/.

ACKNOWLEDGMENTS

We are grateful to M. Bregni and C. Bordignon for helpful discussions; A. Mondino and R. Hess Michelini for help with T cell studies; L. Sergi Sergi for vector production; M. Ponzoni and F. Sanvito for assistance with pathology; and L. Persano, M. Masiero, and E. Hauben for help with some experiments. This research was supported by grants from the Associazione Italiana per la Ricerca sul Cancro (AIRC), the European Union (FP6 Tumor-Host Genomics), and Telethon to L.N.

Received: March 31, 2007
Revised: June 27, 2008
Accepted: September 15, 2008
Published: October 6, 2008

REFERENCES

Aboody, K.S., Najbauer, J., and Danks, M.K. (2008). Stem and progenitor cell-mediated tumor selective gene therapy. Gene Ther. *15*, 739–752.

Ahn, G.O., and Brown, J.M. (2008). Matrix metalloproteinase-9 is required for tumor vasculogenesis but not for angiogenesis: role of bone marrow-derived myelomonocytic cells. Cancer Cell *13*, 193–205.

Balkwill, F.R., and Proietti, E. (1986). Effects of mouse interferon on human tumour xenografts in the nude mouse host. Int. J. Cancer *38*, 375–380.

Belardelli, F., Ferrantini, M., Proietti, E., and Kirkwood, J.M. (2002). Interferon-alpha in tumor immunity and immunotherapy. Cytokine Growth Factor Rev. *13*, 119–134.

Blankenstein, T. (2005). The role of tumor stroma in the interaction between tumor and immune system. Curr. Opin. Immunol. *17*, 180–186.

Bordignon, C. (2006). Stem-cell therapies for blood diseases. Nature *441*, 1100–1102.

Brassard, D.L., Grace, M.J., and Bordens, R.W. (2002). Interferon-alpha as an immunotherapeutic protein. J. Leukoc. Biol. *71*, 565–581.

Brown, B.D., Venneri, M.A., Zingale, A., Sergi Sergi, L., and Naldini, L. (2006). Endogenous microRNA regulation suppresses transgene expression in hematopoietic lineages and enables stable gene transfer. Nat. Med. *12*, 585–591.

Condeelis, J., and Pollard, J.W. (2006). Macrophages: obligate partners for tumor cell migration, invasion, and metastasis. Cell *124*, 263–266.

Curnis, F., Gasparri, A., Sacchi, A., Cattaneo, A., Magni, F., and Corti, A. (2005). Targeted delivery of IFNgamma to tumor vessels uncouples antitumor from counterregulatory mechanisms. Cancer Res. *65*, 2906–2913.

Deininger, M.H., Meyermann, R., and Schluesener, H.J. (2002). The allograft inflammatory factor-1 family of proteins. FEBS Lett. *514*, 115–121.

De Palma, M., and Naldini, L. (2002). Transduction of a gene expression cassette using advanced generation lentiviral vectors. Methods Enzymol. *346*, 514–529.

De Palma, M., and Naldini, L. (2006). Role of haematopoietic cells and endothelial progenitors in tumour angiogenesis. Biochim. Biophys. Acta *1766*, 159–166.

De Palma, M., Venneri, M.A., Roca, C., and Naldini, L. (2003). Targeting exogenous genes to tumor angiogenesis by transplantation of genetically modified hematopoietic stem cells. Nat. Med. *9*, 789–795.

De Palma, M., Montini, E., Santoni de Sio, F.R., Benedicenti, F., Gentile, A., Medico, E., and Naldini, L. (2005a). Promoter trapping reveals significant differences in integration site selection between MLV and HIV vectors in primary hematopoietic cells. Blood *105*, 2307–2315.

De Palma, M., Venneri, M.A., Galli, R., Sergi, L.S., Politi, L.S., Sampaolesi, M., and Naldini, L. (2005b). Tie2 identifies a hematopoietic lineage of proangiogenic monocytes required for tumor vessel formation and a mesenchymal population of pericyte progenitors. Cancer Cell *8*, 211–226.

De Palma, M., Murdoch, C., Venneri, M.A., Naldini, L., and Lewis, C.E. (2007). Tie2-expressing monocytes: regulation of tumor angiogenesis and therapeutic implications. Trends Immunol. *28*, 519–524.

de Visser, K.E., Eichten, A., and Coussens, L.M. (2006). Paradoxical roles of the immune system during cancer development. Nat. Rev. Cancer *6*, 24–37.

Dinney, C.P., Bielenberg, D.R., Perrotte, P., Reich, R., Eve, B.Y., Bucana, C.D., and Fidler, I.J. (1998). Inhibition of basic fibroblast growth factor expression, angiogenesis, and growth of human bladder carcinoma in mice by systemic interferon-alpha administration. Cancer Res. *58*, 808–814.

Du, R., Lu, K.V., Petritsch, C., Liu, P., Ganss, R., Passegue, E., Song, H., Vandenberg, S., Johnson, R.S., Werb, Z., et al. (2008). HIF1alpha induces the recruitment of bone marrow-derived vascular modulatory cells to regulate tumor angiogenesis and invasion. Cancer Cell *13*, 206–220.

Dunn, G.P., Koebel, C.M., and Schreiber, R.D. (2006). Interferons, immunity and cancer immunoediting. Nat. Rev. Immunol. *6*, 836–848.

Fuchs, E.J., and Whartenby, K.A. (2004). Hematopoietic stem cell transplant as a platform for tumor immunotherapy. Curr. Opin. Mol. Ther. *6*, 48–53.

Gresser, I., Bourali, C., Levy, J.P., Fontaine-Brouty-Boye, D., and Thomas, M.T. (1969). Increased survival in mice inoculated with tumor cells and treated with interferon preparations. Proc. Natl. Acad. Sci. USA *63*, 51–57.

Gutterman, J.U. (1994). Cytokine therapeutics: lessons from interferon alpha. Proc. Natl. Acad. Sci. USA *91*, 1198–1205.

Honda, K., Yanai, H., Negishi, H., Asagiri, M., Sato, M., Mizutani, T., Shimada, N., Ohba, Y., Takaoka, A., Yoshida, N., et al. (2005). IRF-7 is the master regulator of type-I interferon-dependent immune responses. Nature *434*, 772–777.

Husemann, Y., Geigl, J.B., Schubert, F., Musiani, P., Meyer, M., Burghart, E., Forni, G., Eils, R., Fehm, T., Riethmuller, G., et al. (2008). Systemic spread is an early step in breast cancer. Cancer Cell *13*, 58–68.

Jones, N., Iljin, K., Dumont, D.J., and Alitalo, K. (2001). Tie receptors: new modulators of angiogenic and lymphangiogenic responses. Nat. Rev. Mol. Cell Biol. *2*, 257–267.

Kouros-Mehr, H., Bechis, S.K., Slorach, E.M., Littlepage, L.E., Egeblad, M., Ewald, A.J., Pai, S.Y., Ho, I.C., and Werb, Z. (2008). GATA-3 links tumor differentiation and dissemination in a luminal breast cancer model. Cancer Cell *13*, 141–152.

Lesinski, G.B., Anghelina, M., Zimmerer, J., Bakalakos, T., Badgwell, B., Parihar, R., Hu, Y., Becknell, B., Abood, G., Chaudhury, A.R., et al. (2003). The antitumor effects of IFN-alpha are abrogated in a STAT1-deficient mouse. J. Clin. Invest. *112*, 170–180.

Lin, E.Y., Nguyen, A.V., Russell, R.G., and Pollard, J.W. (2001). Colony-stimulating factor 1 promotes progression of mammary tumors to malignancy. J. Exp. Med. *193*, 727–740.

Lin, E.Y., Jones, J.G., Li, P., Zhu, L., Whitney, K.D., Muller, W.J., and Pollard, J.W. (2003). Progression to malignancy in the polyoma middle T oncoprotein mouse breast cancer model provides a reliable model for human diseases. Am. J. Pathol. *163*, 2113–2126.

Ljungman, P., Urbano-Ispizua, A., Cavazzana-Calvo, M., Demirer, T., Dini, G., Einsele, H., Gratwohl, A., Madrigal, A., Niederwieser, D., Passweg, J., et al. (2006). Allogeneic and autologous transplantation for haematological diseases, solid tumours and immune disorders: definitions and current practice in Europe. Bone Marrow Transplant. *37*, 439–449.

Lucas, M., Schachterle, W., Oberle, K., Aichele, P., and Diefenbach, A. (2007). Dendritic cells prime natural killer cells by trans-presenting interleukin 15. Immunity *26*, 503–517.

Openshaw, P., Murphy, E.E., Hosken, N.A., Maino, V., Davis, K., Murphy, K., and O'Garra, A. (1995). Heterogeneity of intracellular cytokine synthesis at the single-cell level in polarized T helper 1 and T helper 2 populations. J. Exp. Med. *182*, 1357–1367.

Parmar, S., and Platanias, L.C. (2003). Interferons: mechanisms of action and clinical applications. Curr. Opin. Oncol. *15*, 431–439.

Pfeffer, L.M. (1997). Biologic activities of natural and synthetic type I interferons. Semin. Oncol. *24* (*Suppl 9*), S9–S63.

Salmon, P., Le Cotonnec, J.Y., Galazka, A., Abdul-Ahad, A., and Darragh, A. (1996). Pharmacokinetics and pharmacodynamics of recombinant human interferon-beta in healthy male volunteers. J. Interferon Cytokine Res. *16*, 759–764.

Shaked, Y., Emmenegger, U., Man, S., Cervi, D., Bertolini, F., Ben-David, Y., and Kerbel, R.S. (2005). Optimal biologic dose of metronomic chemotherapy regimens is associated with maximum antiangiogenic activity. Blood *106*, 3058–3061.

Shojaei, F., Zhong, C., Wu, X., Yu, L., and Ferrara, N. (2008). Role of myeloid cells in tumor angiogenesis and growth. Trends Cell Biol. *18*, 372–378.

Sidky, Y.A., and Borden, E.C. (1987). Inhibition of angiogenesis by interferons: effects on tumor- and lymphocyte-induced vascular responses. Cancer Res. *47*, 5155–5161.

Slaton, J.W., Perrotte, P., Inoue, K., Dinney, C.P., and Fidler, I.J. (1999). Interferon-alpha-mediated down-regulation of angiogenesis-related genes and therapy of bladder cancer are dependent on optimization of biological dose and schedule. Clin. Cancer Res. *5*, 2726–2734.

Solorzano, C.C., Hwang, R., Baker, C.H., Bucana, C.D., Pisters, P.W., Evans, D.B., Killion, J.J., and Fidler, I.J. (2003). Administration of optimal biological dose and schedule of interferon alpha combined with gemcitabine induces apoptosis in tumor-associated endothelial cells and reduces growth of human pancreatic carcinoma implanted orthotopically in nude mice. Clin. Cancer Res. *9*, 1858–1867.

Stark, G.R., Kerr, I.M., Williams, B.R., Silverman, R.H., and Schreiber, R.D. (1998). How cells respond to interferons. Annu. Rev. Biochem. *67*, 227–264.

Stetson, D.B., and Medzhitov, R. (2006). Type I interferons in host defense. Immunity *25*, 373–381.

Theofilopoulos, A.N., Baccala, R., Beutler, B., and Kono, D.H. (2005). Type I interferons (alpha/beta) in immunity and autoimmunity. Annu. Rev. Immunol. *23*, 307–336.

Tosi, D., Valenti, R., Cova, A., Sovena, G., Huber, V., Pilla, L., Arienti, F., Belardelli, F., Parmiani, G., and Rivoltini, L. (2004). Role of cross-talk between IFN-alpha-induced monocyte-derived dendritic cells and NK cells in priming CD8+ T cell responses against human tumor antigens. J. Immunol. *172*, 5363–5370.

Venneri, M.A., De Palma, M., Ponzoni, M., Pucci, F., Scielzo, C., Zonari, E., Mazzieri, R., Doglioni, C., and Naldini, L. (2007). Identification of proangiogenic TIE2-expressing monocytes (TEMs) in human peripheral blood and cancer. Blood *109*, 5276–5285.

Vigna, E., Amendola, M., Benedicenti, F., Simmons, A.D., Follenzi, A., and Naldini, L. (2005). Efficient Tet-dependent expression of human factor IX in vivo by a new self-regulating lentiviral vector. Mol. Ther. *11*, 763–775.

Willimsky, G., and Blankenstein, T. (2007). The adaptive immune response to sporadic cancer. Immunol. Rev. *220*, 102–112.